PCCP

PAPER

View Article Online
View Journal | View Issue

Cite this: *Phys. Chem. Chem. Phys.*, 2016, **18**, 7075

The effect of electrolyte composition on the electroreduction of CO_2 to CO on Ag based gas diffusion electrodes†

Sumit Verma,[ab] Xun Lu,[a] Sichao Ma,[bc] Richard I. Masel[d] and Paul J. A. Kenis*[ab]

Received 21st September 2015,
Accepted 20th November 2015

DOI: 10.1039/c5cp05665a

www.rsc.org/pccp

The electroreduction of CO_2 to C_1–C_2 chemicals can be a potential strategy for utilizing CO_2 as a carbon feedstock. In this work, we investigate the effect of electrolytes on the electroreduction of CO_2 to CO on Ag based gas diffusion electrodes. Electrolyte concentration was found to play a major role in the process for the electrolytes (KOH, KCl, and $KHCO_3$) studied here. Several fold improvements in partial current densities of CO (j_{CO}) were observed on moving from 0.5 M to 3.0 M electrolyte solution independent of the nature of the anion. j_{CO} values as high as 440 mA cm^{-2} with an energy efficiency (EE) of $\approx$ 42% and 230 mA cm^{-2} with EE $\approx$ 54% were observed when using 3.0 M KOH. Electrochemical impedance spectroscopy showed that both the charge transfer resistance (R_{ct}) and the cell resistance (R_{cell}) decreased on moving from a 0.5 M to a 3.0 M KOH electrolyte. Anions were found to play an important role with respect to reducing the onset potential of CO in the order OH^- (−0.13 V *vs.* RHE) < HCO_3^- (−0.46 V *vs.* RHE) < Cl^- (−0.60 V *vs.* RHE). A decrease in R_{ct} upon increasing electrolyte concentration and the effect of anions on the cathode can be explained by an interplay of different interactions in the electrical double layer that can either stabilize or destabilize the rate limiting $CO_2^{\bullet-}$ radical. EMIM based ionic liquids and 1 : 2 choline Cl urea based deep eutectic solvents (DESs) have been used for CO_2 capture but exhibit low conductivity. Here, we investigate if the addition of KCl to such solutions can improve conductivity and hence j_{CO}. Electrolytes containing KCl in combination with EMIM Cl, choline Cl, or DESs showed a two to three fold improvement in j_{CO} in comparison to those without KCl. Using such mixtures can be a strategy for integrating the process of CO_2 capture with CO_2 conversion.

Introduction

Carbon dioxide (CO_2) levels in the atmosphere have risen from 320 to more than 400 ppm in the past 50 years.[1] In a recent paper Feldman *et al.* provided the first experimental evidence of how rising CO_2 levels are affecting the Earth's surface energy balance leading to an adverse environmental impact.[2] Simultaneous implementation of multiple approaches has been proposed to mitigate the negative effects of high global CO_2 emissions.[3] These include switching from traditional fossil fuel power plants to renewable energy sources, increasing the energy efficiency of vehicles and buildings, and the capture and sequestration of CO_2. The electrocatalytic conversion of CO_2 into value added chemicals and fuels could also be an important means of reducing CO_2 emissions.[4–8] Depending on the catalyst, electrolyte, and reaction conditions being used,[9,10] different products such as methanol (CH_3OH),[11–13] formic acid (HCOOH),[14–17] and carbon monoxide (CO)[18–23] are formed. Furthermore, this approach can also be used to store otherwise wasted excess energy from renewable sources when supply exceeds demand.

In this work, we focus on the electrocatalytic conversion of CO_2 to CO in an electrochemical flow reactor developed earlier in our group.[14] CO is an important carbon intermediate used for the production of chemicals such as acetic acid,[24] phosgene,[25] and aldehydes.[26] Furthermore, mixtures of H_2 and CO ("syngas") can be used to produce higher hydrocarbons and combustion fuels *via* the Fischer–Tropsch process.[27,28] Although the standard reduction potential for the conversion of CO_2 to CO is low (*i.e.*, −0.109 V *vs.* SHE at pH = 0), the reaction suffers from high activation overpotential.[10,29] The reason for such a high overpotential is often attributed to the high equilibrium potential associated with the formation of the radical intermediate $CO_2^{\bullet-}$ during the first step of the reaction.[30] This reaction proceeds with an equilibrium potential value of −1.9 V *vs.* SHE.[31]

[a] *Department of Chemical & Biomolecular Engineering, University of Illinois at Urbana-Champaign, 600 South Mathews Avenue, Urbana, Illinois 61801, USA. E-mail: kenis@illinois.edu*
[b] *International Institute for Carbon Neutral Energy Research (WPI-I2CNER), Kyushu University, 744 Motooka, Nishi-ku, Fukuoka 819-0395, Japan*
[c] *Department of Chemistry, University of Illinois at Urbana-Champaign, 505 South Mathews Avenue, Urbana, Illinois 61801, USA*
[d] *Dioxide Materials, 3998 FAU Boulevard #300, Boca Raton, Florida 33431, USA*

† Electronic supplementary information (ESI) available. See DOI: 10.1039/c5cp05665a

Starting with the seminal work of Hori *et al.*[32] that pointed out Au, Ag, and Zn to be active for this reaction, a lot of cathode catalysts have been reported.[18–20,22,33] In prior work, we as well as others have studied Ag catalysts with respect to the electroreduction of CO_2 to CO.[21,34–36] We have also looked at the effect of the catalyst layer deposition method on electrode preparation,[37] and the effect of support materials such as TiO_2 on this electrochemical reaction.[23]

Electrolytes have been shown to play a major role in the electroreduction of CO_2 to CO. For example, Rosen *et al.* proposed the use of an ionic liquid electrolyte 1-ethyl-3-methylimidazolium tetrafluoroborate (EMIM BF_4) as a co-catalyst to stabilize the radical intermediate $CO_2^{\bullet -}$.[38] CO was formed at an onset cell potential of −1.5 V, much lower than the onset potential observed when using electrolytes such as aqueous KCl or acetonitrile (nearly −2.2 V). Sun *et al.* showed that the addition of ionic liquid 1-ethyl-3-methylimidazolium bis(trifluouromethylsulfonyl)imide (EMIM TF_2N) lowered the reduction potential and favored the formation of CO over oxalate when using Pb on the cathode.[39] Zhu *et al.* used choline chloride (choline Cl) to suppress hydrogen (H_2) formation and lower the reduction potential of bicarbonate (HCO_3^-) to CO.[40] However, in most of the ionic liquid related work, the partial current density of CO (j_{CO}) was typically low (less than 5 mA cm^{-2}). This observation was attributed to the low ionic conductivity of such solutions.[38] Several others have used EMIM based ionic liquids and choline Cl based deep eutectic solvents (DESs) for post combustion CO_2 capture as well.[41–43]

In other work, Thorson *et al.* investigated the influence of several different alkali cations on the electroreduction of CO_2 to CO.[44] Analysis of the Faradaic efficiencies suggested that larger cations suppressed H_2 evolution while favoring CO_2 reduction. Earlier Hori *et al.* showed that the choice of the cation for bicarbonate electrolytes can severely change the distribution of products on Cu cathodes.[45] Wu *et al.* reported a difference in activity and selectivity of Sn electrodes when different electrolytes such as K_2SO_4, KCl, or $NaHCO_3$ were used.[46]

Here, we attempt to further understand the effect of electrolytes on the electroreduction of CO_2 to CO. We first look at how changing the electrolyte concentration affects j_{CO}. We then investigate the effect of anions on onset potentials and j_{CO} for this reaction. Using electrochemical impedance spectroscopy (EIS), we try to provide mechanistic insights into the effect of electrolyte concentration and anions on the reaction. Subsequently, we design and explore a combination of EMIM Cl, choline Cl, and a choline Cl based DES (1 : 2 choline Cl urea mixture) with KCl to develop a strategy to improve j_{CO} for ionic liquid and DES based electrolytes by improving their conductivity. Such an electrolyte mixture can be used for integrating the process of CO_2 capture with CO_2 conversion.

Experimental

Preparation of electrodes

The cathodes were prepared by spraying the catalyst ink on a Sigracet 35 BC gas diffusion layer (GDL) electrode (Ion Power Inc.) using an automated air-brush setup.[37] Four cathodes were made at a time. Unsupported Ag nanoparticles (<100 nm, 99.5% trace metal basis, Sigma Aldrich) were used as the catalyst. The catalyst ink was prepared by mixing 42 mg of Ag with 1600 μL of E-pure water (>17.9 MΩ cm), 55 μL of Nafion solution (5 wt%, Fuel Cell Earth), and 1600 μL of isopropyl alcohol. The mixture was then sonicated (Vibra-Cell ultrasonic processor, Sonics & Materials) for 20 minutes. The resulting solution was then airbrushed onto a GDL with a geometric area of 5 × 2 cm^2. The actual catalyst loading was determined by weighing the GDL before and after deposition. Anodes were prepared by hand painting a mixture of 4.5 mg IrO_2 non-hydrate (99.99% metals basis, Ir 84.5% min, Alfa-Aeser), 200 μL of E-pure water (>17.9 MΩ cm), 15 μL of Nafion solution (5 wt%, Fuel Cell Earth), and 200 μL of isopropyl alcohol on a Sigracet 35 BC gas diffusion layer (GDL) electrode (Ion Power Inc.) with a geometric area of 2.5 × 0.8 cm^2. Hand painting was done using a paintbrush. The GDL was weighed before and after painting to determine the actual catalyst loading. All the cathodes had a final loading of 2 ± 0.1 mg cm^{-2} Ag and all anodes had a final loading of 2 ± 0.1 mg cm^{-2} IrO_2.

Preparation of electrolytes

All salts were purchased and used without any further purification. Different concentrations and compositions of electrolytes were prepared by dissolving the appropriate amount of salt in E-Pure water (>17.9 MΩ cm) to get a final solution volume of 100 mL. The following salts were used: KCl (product number: BP366, purity: 99.0% min, supplier: Fischer Scientific), KOH (product number: P250, purity: assay 86.3%, supplier: Fischer Scientific), $KHCO_3$ (product number: 237205, purity: 99.7% granular, supplier: Sigma Aldrich), EMIM Cl (product number: IL-0093, purity: >98%, supplier: Iolitec), choline Cl (product number: C1879, purity: >98%, supplier: Sigma Aldrich), and urea (product number: 8648-04, purity: >99%, supplier: Macron Fine Chemicals). The conductivity and pH of the electrolytes were measured using an Orion 4 star pH-conductivity meter at 20 °C when required.

Operation of an electrochemical flow reactor

A slightly modified version of the flow reactor reported earlier by us was used for the electrochemical experiments.[14] The only difference in the new design from the old was that we replaced the graphite current collector and the aluminium anode with a single stainless steel anode current collector. Similar to our previous design, a mass flow controller (Smart Trak 2, Sierra Instruments) was used to flow CO_2 gas (S.J. Smith Welding Supply) at a set flow rate of 17 sccm over the cathode GDL. High flow rates were used in order to avoid mass transfer limitations and the issue of CO_2 solubility in the electrolyte. The strategy resulted in a dilution of the H_2 concentration in the effluent gas stream, which helps it in being analysed accurately by a He carrier gas. A syringe pump (PHD 2000, Harvard Apparatus) was used to pump the electrolyte between the cathode and the anode at a flow rate of 0.5 mL min^{-1}. A pressure controller (Cole Parmer, 00268TC) was used to maintain low pressure

(14.20 psig) in the downstream of the reactor to facilitate easier transfer of the gas products formed on the cathode surface to the effluent gas stream. A potentiostat (Autolab PGSTAT-30, EcoChemie) was used to carry out the electrochemical reaction. Experiments were performed in the potentiostatic electrolysis mode and under ambient conditions. A fresh cathode and a fresh anode were used for all experiments. After stepping on to a potential, the current was stabilized for at least 180 seconds before the gas analysis was performed. The gaseous product stream was analysed by sampling 1 mL of the effluent gas stream diverted into the gas chromatograph (Thermo Finnigan Trace GC) operating in the thermal conductivity detection (TCD) mode, with a Carboxen 1000 column (Supelco) and Helium as the carrier gas at a flow rate of 20 sccm. The column was held at 150 °C and the TCD detector at 200 °C. Liquid products were not analysed for this reaction. Since GDL electrodes were being used as the electrodes, fluctuations in current densities were observed due to gas bubbling. Current was averaged over a time period of 240 seconds after the gas analysis was started. A triple injection was used to average out the gaseous product peaks over time. Error bars on the different plots represent errors due to the difference in the three injections and the fluctuations in current density. Individual electrode potential was recorded using a multimeter (AMPROBE 15XP-B) connected between the electrode and the reference electrode (Ag/AgCl; 3 mol kg^{-1} KCl, RE-5B, BASi) as shown in our previous work.[47] The reference electrode was placed in the inlet stream of the electrolyzer to avoid the effect of any pH changes (summarized in Table S1, ESI†) that occur in the flow cell as a function of electrolyte, cathode potential, and current density. All electrode potentials were converted to RHE according to the Nernst equation ($E_{RHE} = 0.210 + E_{Ag/AgCl} + 0.059 \times pH$).

Electrochemical impedance spectroscopy

Electrochemical impedance spectroscopy was performed on the flow cell using the frequency response module of the potentiostat (Autolab PGSTAT-30, EcoChemie). The spectrum was recorded in a potentiostatic mode at a cell potential of −2.00 V or −2.25 V. Higher potentials were not used as a significant amount of noise in the data was obtained due to gas bubbling at the GDL. Moreover, at lower cell potentials charge transfer plays a more important role than the conductivity of the electrolyte solution

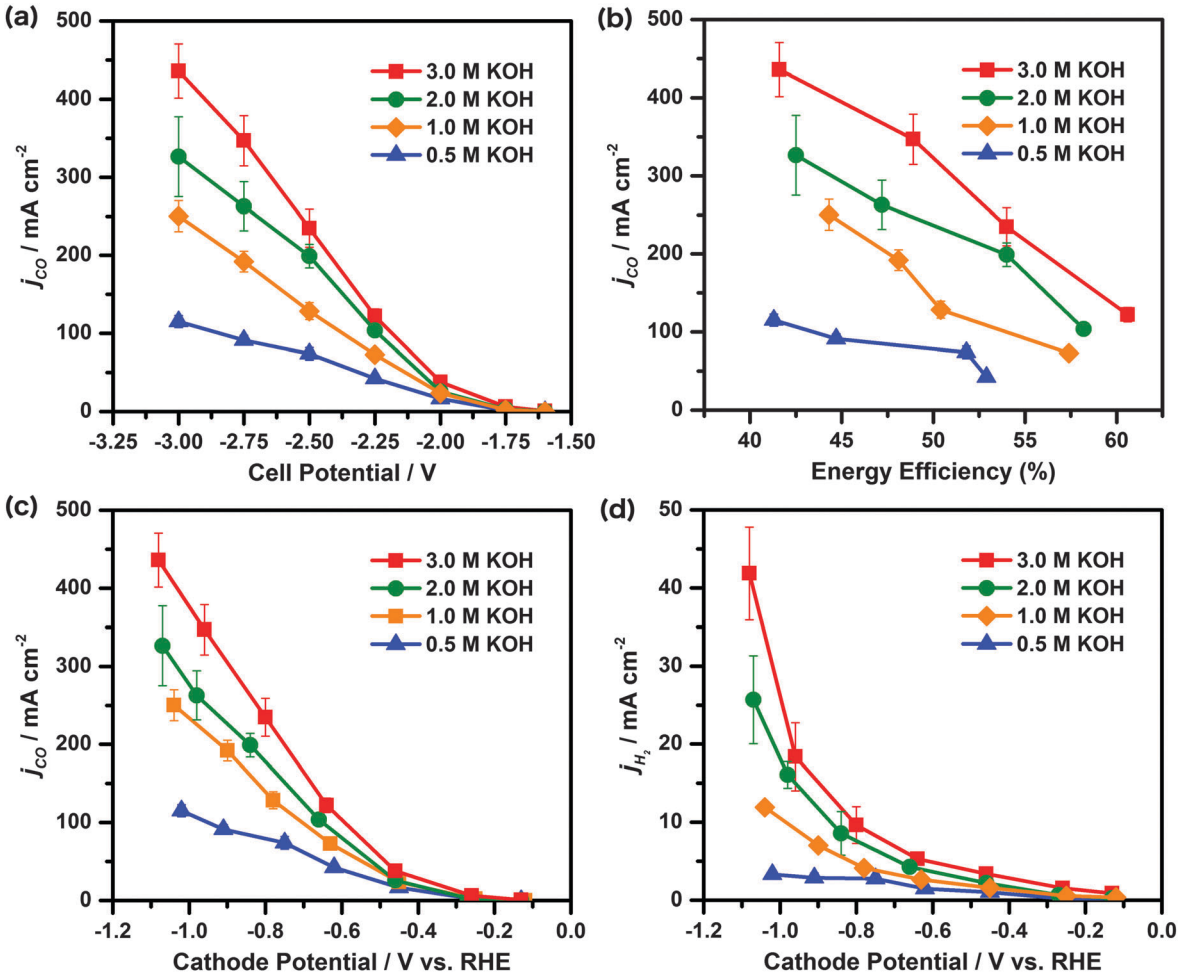

Fig. 1 Partial current density of CO as a function of (a) cell potential, (b) energy efficiency, and (c) cathode potential, as well as (d) partial current density of H_2 as a function of cathode potential for four different KOH electrolyte concentrations when using Ag nanoparticles as the cathode catalyst and IrO_2 as the anode catalyst.

and hence a better understanding of kinetics can be obtained. 100 different frequencies (range: 10 kHz to 0.1 Hz) were used to scan the system in a logarithmic step. A single sine wave with an amplitude of 10 mV was used for the sweep. The high frequency intercept on the *x*-axis of the Nyquist plot represents the internal resistance of the cell (R_{cell}), which includes the contact resistance and the solution resistance. The diameter of the semi-circle represents the charge transfer resistance (R_{ct}) for the reaction.

Results and discussion

Effect of electrolyte concentration

The effect of electrolyte concentration on electrochemical CO_2 reduction was studied by utilizing different concentrations of aqueous KOH as the electrolyte: 0.5, 1.0, 2.0, and 3.0 M (Fig. 1). Almost a four-fold improvement in j_{CO} was observed on going from 0.5 M to 3.0 M KOH at a cell potential of −3.00 V (Fig. 1(a)). Similar trends were observed with respect to the cathode potential (Fig. 1(c)). A j_{CO} as high as 440 mA cm^{-2} was obtained at an energetic efficiency of 42% (calculated using a method described earlier[6]), while an energy efficiency of 54% can be obtained in combination with a j_{CO} of 230 mA cm^{-2} (Fig. 1(b)). To the best of our knowledge the j_{CO} values reported here are some of the highest reported in the literature when operating under ambient conditions. Other work showing similar current density levels (up to 300 mA cm^{-2}) was performed at high pressures (>15 atm) and high overall cell potentials (more negative than −3.00 V).[36]

To confirm whether the observed trend of improving j_{CO} with increasing electrolyte concentration is a more general phenomenon, we carried out experiments with aqueous electrolytes containing different concentrations of KCl and $KHCO_3$. A similar trend of increasing j_{CO} upon increasing electrolyte concentration was observed in all cases independent of the nature of the anion (Fig. 2). Min *et al.*[48] and Murata *et al.*[49] had earlier observed this phenomenon for $KHCO_3$. They explained this behavior by indicating that an increase in the concentration of HCO_3^- ions removed OH^- formed in the process thereby shifting the reaction equilibrium to favor CO production. Although, this might be a possible explanation for the case

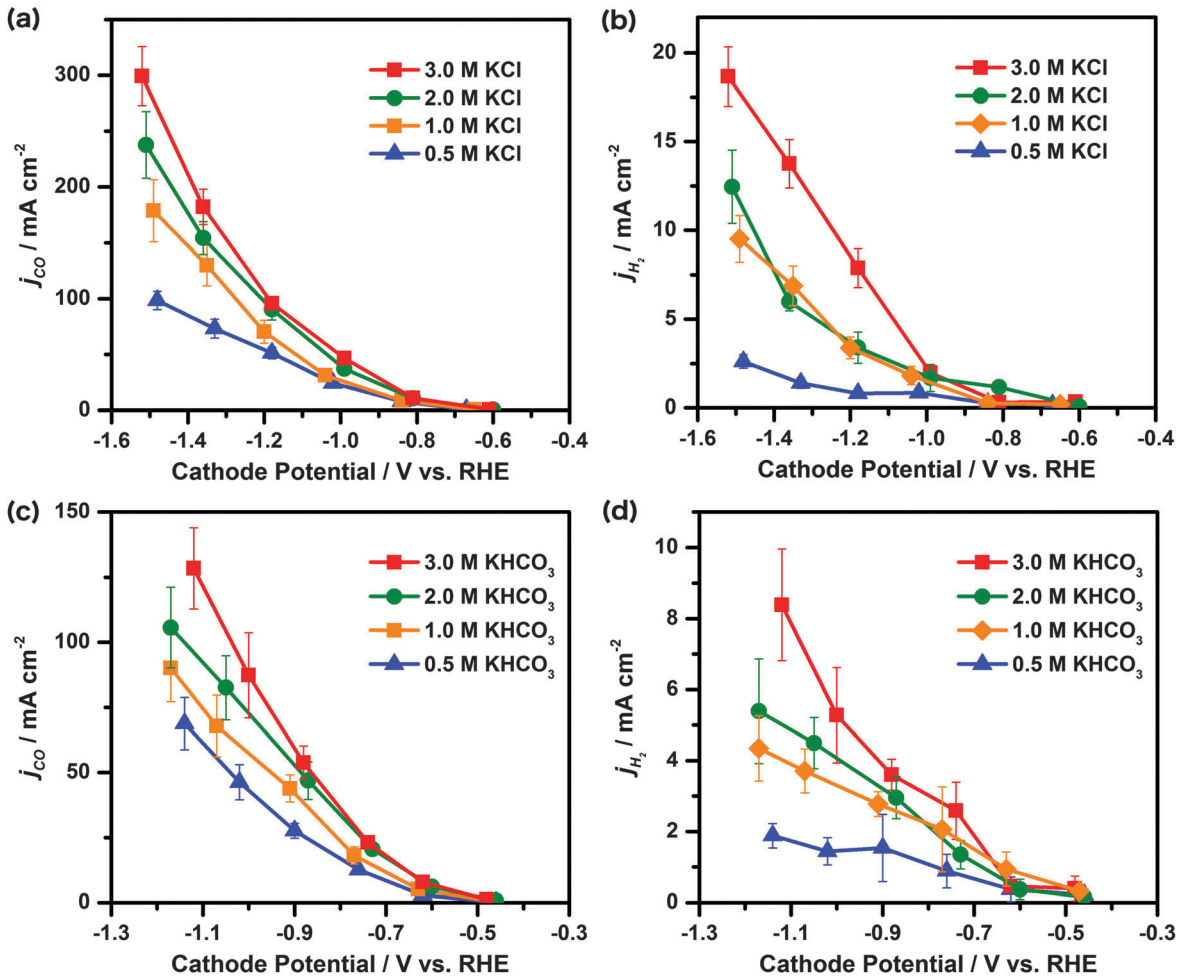

Fig. 2 Partial current density of CO and H_2 using 4 different electrolyte concentrations of (a and b) KCl and (c and d) $KHCO_3$ when using Ag nanoparticles as the cathode catalyst and IrO_2 as the anode catalyst.

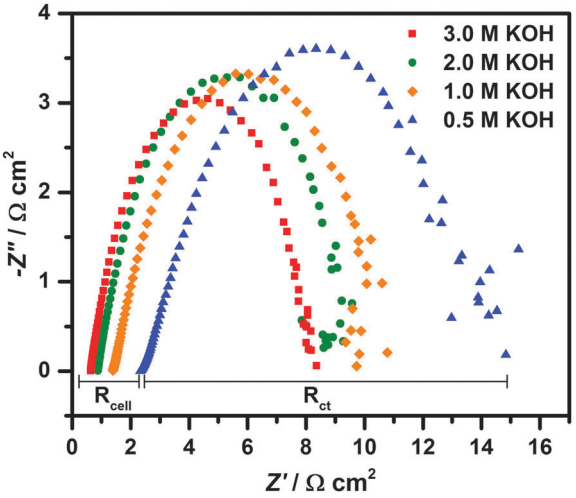

Fig. 3 Nyquist plot for different electrolytes obtained *via* electrochemical impedance spectroscopy at a cell potential of −2.00 V.

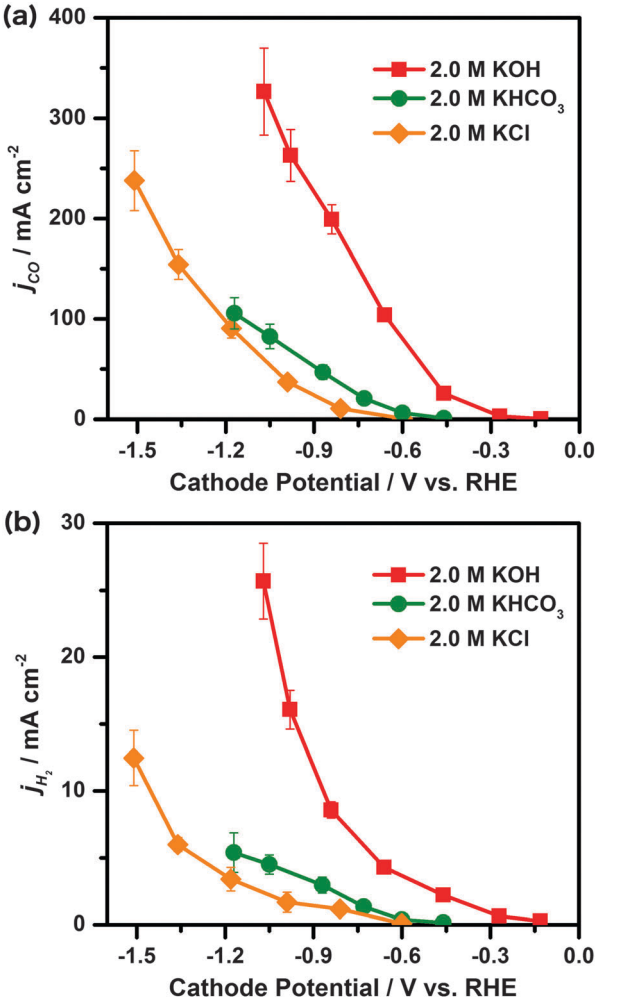

Fig. 4 Partial current density of (a) CO and (b) H_2 obtained using different electrolytes and when using Ag nanoparticles as the cathode catalyst and IrO_2 as the anode catalyst.

of $KHCO_3$, our results indicate that the improvement in j_{CO} is independent of the nature of the anion and therefore a more general factor might be at play here.

To gain further mechanistic insights into the observed phenomena, we performed electrochemical impedance spectroscopy on the electrochemical flow reactor at a cell potential of −2.00 V using different concentrations of KOH as the electrolyte. Increasing the electrolyte concentration leads to a reduction in both R_{cell} and R_{ct} (Fig. 3). The observed reduction in R_{cell} can be explained by the improvement in ionic conductivity upon increasing the ionic concentration of the electrolyte. Since the improvement in j_{CO} was independent of the nature of the anion, the observed reduction in R_{ct} potentially could be attributed to an improved stabilization of the rate limiting $CO_2^{\bullet-}$ radical intermediate by a higher concentration of K^+ ions in the outer Helmholtz plane (OHP) of the electrical double layer. Prior work suggests that K^+ can act as a co-catalyst by forming ion pairs or ion bridges with the $CO_2^{\bullet-}$ radical thereby stabilizing it.[50] Cations have also been shown to stabilize anionic or even neutral intermediates in a similar fashion for certain other electrocatalytic reactions.[51,52] Higher concentrations of K^+ and OH^- will lead to a more compact double layer at the electrode–electrolyte interface leading to a smaller Debye length or an OHP closer to the electrode surface.[53] In an analogous fashion, in the area of heterogeneous catalysis, alkali metal amalgams have been shown to catalyze the gas phase reduction of CO_2 to CO by forming complexes with the reacting CO_2 species.[54,55]

Effect of anions

In many electrocatalytic reactions, the anions present in the electrolyte also play an important role. However, the role of anions in the electroreduction of CO_2 has not been explored extensively. To study the effect of anions, we compared the *i*–*V* curves for 2.0 M KOH, 2.0 M KCl, and 2.0 M $KHCO_3$ (Fig. 4). The onset potential observed here for the reduction of CO_2 to CO was found to vary in the order OH^- (−0.13 V *vs.* RHE) < HCO_3^- (−0.46 V *vs.* RHE) < Cl^- (−0.60 V *vs.* RHE) (Fig. 4(a)), which corresponds to overpotentials of 0.02 V, 0.35 V, and 0.49 V, respectively, for these three electrolytes. An improvement in electrochemical performance while using KOH is consistent with prior work.[56,57] The Faradaic efficiency and j_{CO} were observed to vary in the order of OH^- > HCO_3^- > Cl^- (Table 1). In most cases, the sum of the Faradaic efficiencies of CO and H_2 was >85%. HCOOH along with minor liquid products (CH_3OH, C_2H_5OH), and minor gaseous products (CH_4) should constitute the other 15%.[29] Electrochemical impedance spectroscopy carried out at a cell potential of −2.25 V reveals an order of magnitude difference between the observed R_{ct} values of KOH and of KCl, while the R_{ct} value of HCO_3^- resides in between (Fig. 5). The ratio of R_{ct} between KCl and KOH (≈80) is approximately equal to the ratio of j_{total} between the two at a cell potential of −2.25 V. As explained initially by Hori *et al.*[10] and also demonstrated by us later,[58] one of the most important roles of the anion is to modulate surface pH (*i.e.*, act as a buffer), which in turn limits the availability of protons on the surface, thereby increasing the number of active sites available for the

Table 1 Total current density (j_{total}), cathode potential and Faradaic efficiencies (FE) for both CO and H_2 for different concentrations of KOH, $KHCO_3$ and KCl at cell potentials of −2.50 V and −2.75 V

			Cell potential = −2.50 V				Cell potential = −2.75 V			
Electrolyte	Conc. (M)	pH	Cathode potential (*vs.* RHE)	j_{total} (mA cm^{-2})	FE_{CO} (%)	FE_{H_2} (%)	Cathode potential (*vs.* RHE)	j_{total} (mA cm^{-2})	FE_{CO} (%)	FE_{H_2} (%)
KOH	0.5	13.23	−0.75	76.1	97.4	3.6	−0.91	98.7	92.5	2.9
	1.0	13.54	−0.78	135.7	94.8	3.1	−0.90	193.1	99.5	3.6
	2.0	13.77	−0.84	196.0	101.6	4.4	−0.98	269.3	97.6	6.0
	3.0	13.97	−0.80	231.3	101.5	4.2	−0.96	342.8	101.2	5.4
$KHCO_3$	0.5	8.55	−0.76	12.7	99.2	7.0	−0.90	29.5	93.6	5.2
	1.0	8.56	−0.77	22.2	81.4	9.3	−0.91	50.4	87.0	5.5
	2.0	8.59	−0.73	23.5	87.3	5.7	−0.86	55.5	84.4	5.3
	3.0	8.63	−0.74	28.0	82.5	9.2	−0.88	65.6	81.9	5.5
KCl	0.5	6.20	−0.84	8.9	86.3	2.8	−1.02	32.2	75.1	2.6
	1.0	6.32	−0.84	10.1	85.0	2.6	−1.04	39.1	79.6	4.7
	2.0	6.54	−0.81	13.7	77.6	8.5	−0.99	51.4	72.3	3.3
	3.0	6.62	−0.81	14.6	73.6	2.1	−0.99	65.5	71.3	3.0

electroreduction of CO_2 to CO. Such reasoning can help explain the higher j_{CO} and Faradaic efficiencies in the presence of OH^- and HCO_3^- anions as those parameters are directly correlated with the number of available active sites. However, the observed shift in onset potentials cannot be satisfactorily explained by the effect of pH alone. Even though H_2 evolution competes with CO_2 reduction, a few active sites should be available for CO_2 to convert to CO, and hence an onset should be seen. Analogous to these observations for CO_2 reduction, the specific adsorption of anions on the electrode surface has been shown to help stabilize or destabilize key reaction intermediates in the electrocatalytic reduction of O_2 and NO_3^-.[52,59] Smaller anions (such as OH^-) with a large solvation shell tend to interact with the electrode surface only through electrostatic forces and are mostly located beyond the OHP (Fig. 6(a)). Weakly solvated anions (such as Cl^-) on the other hand tend to interact directly (specific adsorption) with the electrode surface (Fig. 6(b)).[60] The Gibbs free energy for the adsorption of Cl^- on a Ag surface is more favourable (−15 kcal mol^{-1}) than Gibbs free energy for OH^- (−3.4 kcal mol^{-1}).[61] Since the specific adsorption of anions plays a major role especially at low potentials,[62] we anticipate that this phenomenon helps cause the observed shift in onset potential for CO_2 reduction. The presence of Cl^- ions on the electrode surface may destabilize the rate limiting $CO_2^{\bullet -}$ species and hence limit CO_2 reduction. The results we report here may appear to deviate from a recent paper that highlights the Cl^- anion favoring CO formation to a greater extent than the HCO_3^- anion.[63] Moreover, the Faradaic efficiencies of CO reported there when using KCl as an electrolyte (<65%) are significantly lower than the values we observe here (>80%) with a similar electrolyte. These differences can probably be attributed

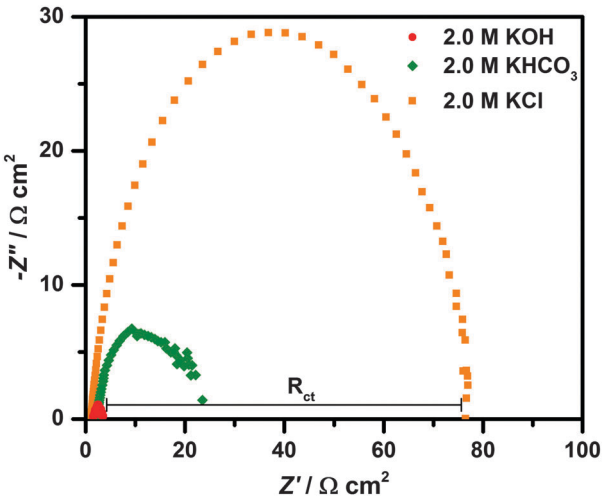

Fig. 5 Nyquist plot for different electrolytes obtained *via* electrochemical impedance spectroscopy at a cell potential of −2.25 V.

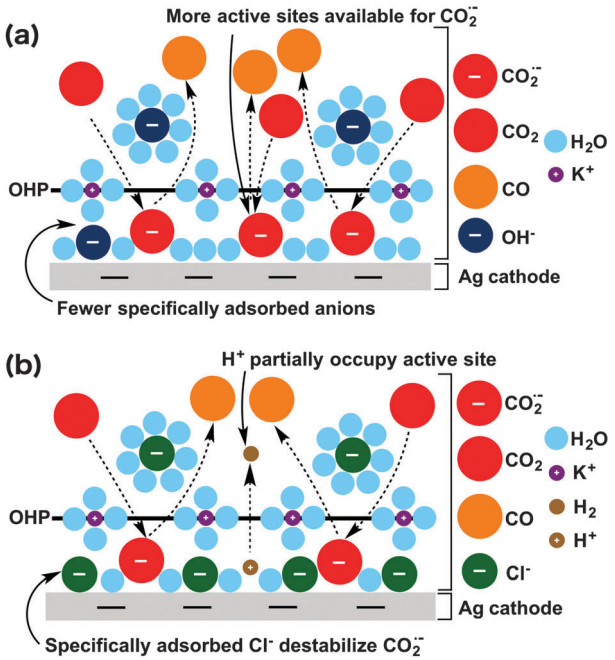

Fig. 6 Schematic illustrations of processes in the double layer that play a role in the kinetics of CO_2 to CO conversion on a Ag cathode when using (a) KOH or (b) KCl as the electrolyte.

Table 2 Total current density (j_{total}), cathodic potential and Faradaic efficiencies (FE) for both CO and H_2 for different mixtures of KCl with EMIM Cl, choline Cl and 1 : 2 choline Cl urea based DESs at cell potentials of −2.50 V and −2.75 V

			Cell potential = −2.50 V				Cell potential = −2.75 V			
Electrolyte	pH	Conductivity (mS cm^{-1})	Cathode potential (*vs.* RHE)	j_{total} (mA cm^{-2})	FE_{CO} (%)	FE_{H_2} (%)	Cathode potential (*vs.* RHE)	j_{total} (mA cm^{-2})	FE_{CO} (%)	FE_{H_2} (%)
2.0 M KCl	6.54	175.0	−0.81	13.7	77.6	8.5	−0.99	51.4	72.3	3.3
2.0 M EMIM Cl	4.48	74.1	−0.86	8.0	91.9	4.3	−1.03	25.0	89.3	1.0
1.5 M KCl + 0.5 M EMIM Cl	5.24	136.0	−0.83	11.5	82.3	27.5	−1.01	42.2	79.6	13.1
2.0 M choline Cl	5.92	74.3	−0.82	8.7	79.9	5.9	−1.00	27.6	78.0	3.3
1.5 M KCl + 0.5 M choline Cl	6.15	142.6	−0.81	13.6	86.6	12.3	−1.00	47.6	85.6	4.0
2.0 M (1 : 2) choline Cl urea	6.45	34.5	−0.68	3.3	81.9	8.9	−0.83	11.6	94.1	1.7
1.5 M KCl + 0.5 M (1 : 2) choline Cl urea	6.52	131.4	−0.72	5.2	81.7	8.4	−0.87	22.1	85.1	4.1

to the use of a different cathode catalyst and preparation method: airbrushed Ag nanoparticles are used in our work, in contrast to *in situ* AgCl-derived Ag nanocorals used in the work reported by Hsieh *et al.* Similar arguments have been reported for a Cu catalyst by Lee *et al.*[64]

Since, in our work, KOH and $KHCO_3$ tend to perform better than KCl, one might argue that CO_3^{2-} or HCO_3^- may be the reacting species. However, earlier work has established that CO_2 is the reacting species and not CO_3^{2-} or HCO_3^-.[65] At higher electrode potentials, the trends in j_{CO} can be explained in terms of the higher electrolyte conductivity of KOH in comparison to the conductivity of the other electrolytes. In addition, since our electrode preparation technique involved the use of Nafion as a binder for the Ag nanoparticle catalyst, we investigated whether sulfonate adsorption plays a role in the electroreduction of CO_2 to CO. Three control experiments, all using a cathode comprised of 2 mg cm^{-2} Ag nanoparticles on a gas diffusion electrode without Nafion and an anode comprised of 2 mg cm^{-2} IrO_2 on a

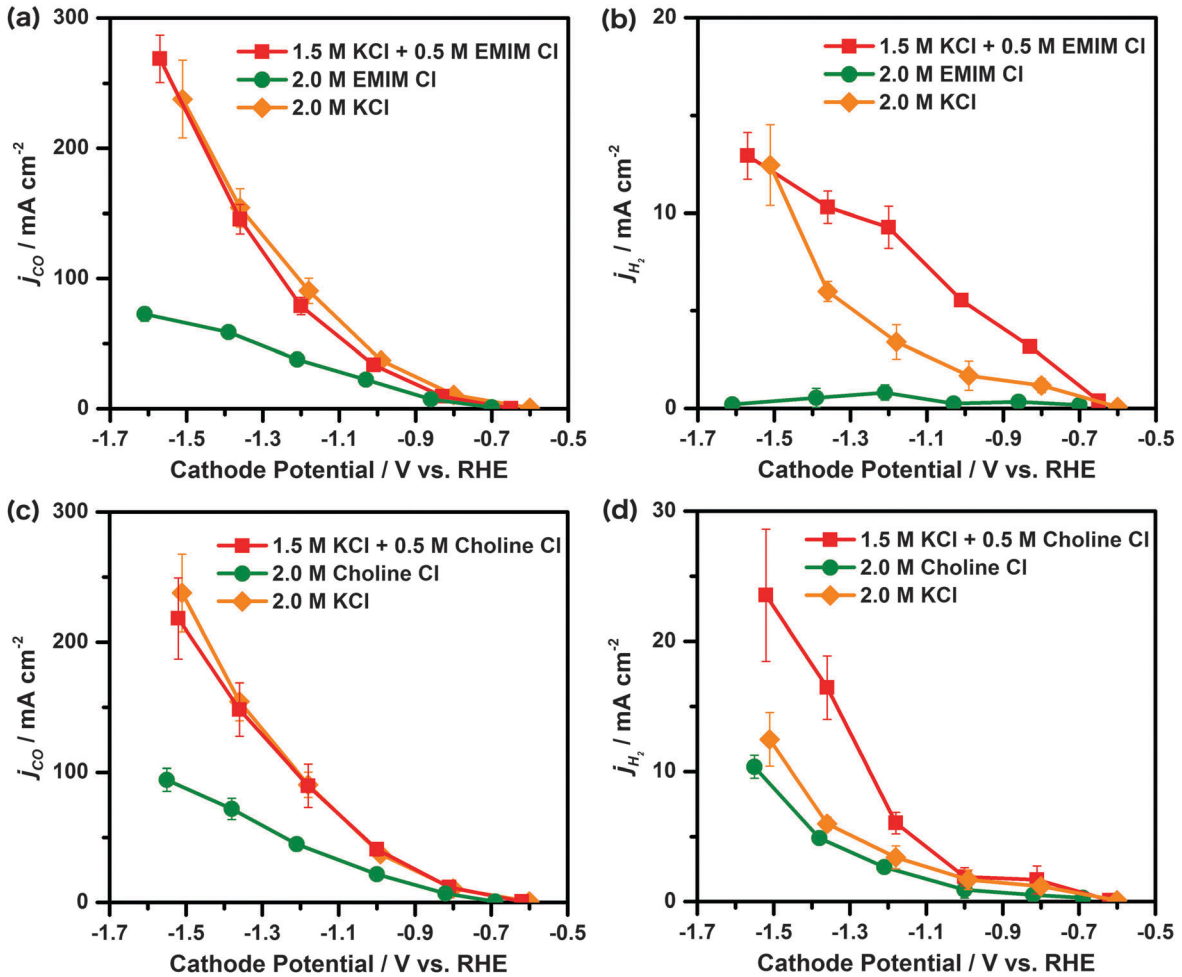

Fig. 7 Partial current density of CO and H_2 obtained using different electrolytes, specifically combinations of KCl with (a and b) EMIM Cl and with (c and d) choline Cl when using Ag nanoparticles as the cathode catalyst and IrO_2 as the anode catalyst.

gas diffusion electrode, were performed using 2.0 M KOH, $KHCO_3$, and KCl, respectively, as the electrolyte. Removing Nafion from the cathode catalyst layer did not have a significant effect on the electrochemical performance in terms of j_{CO} and onset potential when using KCl or $KHCO_3$ as the electrolyte (Fig. S1, ESI†). However, when using KOH as the electrolyte, the onset cathode potential of CO dropped from −0.13 V to −0.08 V *vs.* RHE, which is within the error limits (mainly due to inaccuracy in pH measurements) of the E^0 value of −0.10 V *vs.* RHE for CO production. The fact that the onset is now equal to the standard potential indicates that sulfonate adsorption is important when using KOH as the electrolyte. This observation in turn supports our earlier argument that specific anion adsorption is important for determining the onset potential for the electroreduction of CO_2 to CO.

As shown in our earlier work,[56] electrolytes also affect the chemistries taking place on the anode. When using KOH as the electrolyte, the O_2 evolution reaction takes place at the anode. As a result, OH^- generated at the cathode has a greater chance to get consumed at the anode. Such a continuous removal of the OH^- species from the cathode can enhance CO_2 reduction.

Utilizing mixtures of KCl with EMIM Cl, choline Cl, and choline Cl based DESs

Imidazolium based ionic liquids and choline Cl based deep eutectic solvents (DESs) such as a 1 : 2 mixture of choline Cl and urea are known to be active for CO_2 absorption.[41–43] So, one can imagine using these solutions as electrolytes to combine CO_2 capture with CO_2 conversion. However, one of the biggest drawbacks of these solvents is that their conductivity is low, and hence they exhibit low current densities for electrochemical reactions. To improve the conductivity, we designed aqueous electrolyte mixtures comprised of 1.5 M KCl with 0.5 M of, respectively, EMIM Cl, choline Cl, and DESs (1 : 2 mixture of choline Cl and urea). Since the concentration of the electrolyte plays an important role in the process, the total concentration was kept constant at 2.0 M for all three mixtures. The conductivity of all three mixtures was better than the conductivity of the additives by themselves at 2.0 M concentration (Table 2). A 2 to 3 times improvement in j_{CO} was observed for each mixture in comparison to neat 2.0 M EMIM Cl, 2.0 M choline Cl, and 2.0 M (1 : 2) choline Cl urea DES (Fig. 7 and 8). These j_{CO} values were comparable to j_{CO} obtained with aqueous 2.0 M KCl solution. The Faradaic efficiency of CO was greater for the mixtures when compared to the corresponding values obtained with the 2.0 M KCl electrolyte (Table 2). This is probably due to a greater stabilization of the rate limiting formation of the $CO_2^{\bullet-}$ intermediate by the ammonium species. However, note that at the same time the specific adsorption of ammonium species (when using $EMIM^+$ or $choline^+$) would decrease the number of active sites available for $CO_2^{\bullet-}$. In addition, for j_{CO} values greater than 100 mA cm^{-2}, the electrolyte conductivity starts to play an important role in the process. As a result, the mixtures exhibit j_{CO} values similar to those observed when using the 2.0 M KCl electrolyte. Since the DES combination of choline Cl and urea mixed with KCl performs comparably to the aqueous KCl electrolyte, the strategy of mixing DESs or ionic liquids with a salt of higher conductivity can be used to combine the process of CO_2 capture and conversion.

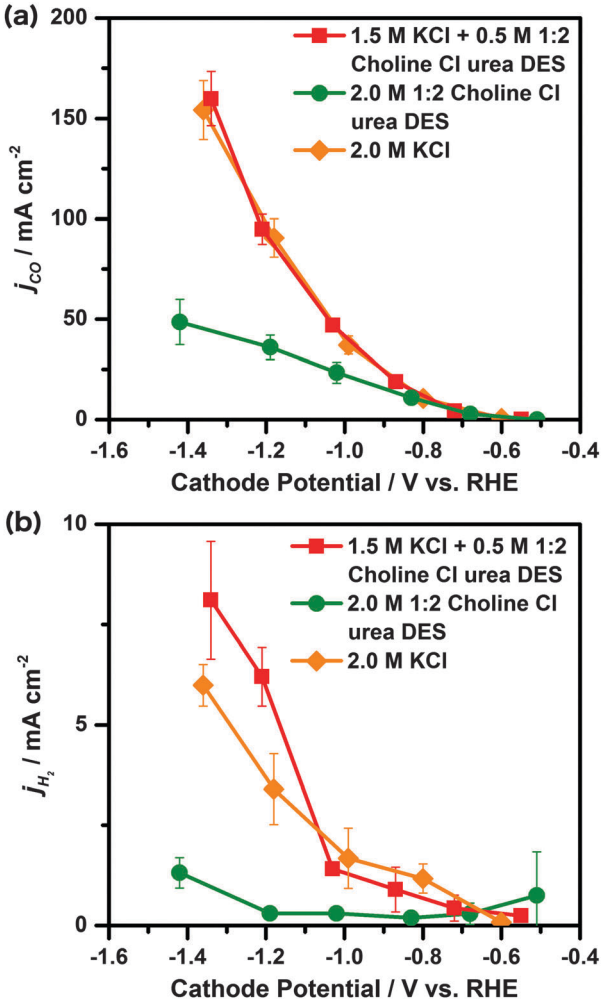

Fig. 8 Comparison of partial current density of (a) CO and (b) H_2 for different electrolytes, including deep eutectic solvents (DESs), when using Ag nanoparticles as the cathode catalyst and IrO_2 as the anode catalyst.

Similar improvements in performance were also observed for mixtures of 2.5 M KCl with 0.5 M of EMIM Cl and DESs (Fig. S2, ESI†). However, the final combination will have to be optimized by balancing the amount of CO_2 that needs to be captured (controlled by EMIM or DES content) with the rate of conversion of CO_2 to CO (controlled by KCl). Furthermore, a rise in pH (from 6.52 to 10.02) was observed when using 1.5 M KCl + 0.5 M 1 : 2 choline Cl urea DES at relatively high j_{CO} (Table S1, ESI†). Such a rise can have a detrimental effect on the stability of these electrolytes as OH^- abstracts the tertiary hydrogen on the ammonium ion responsible for capturing CO_2.[66] As a consequence, the electrolyte would have to be regenerated, *i.e.*, neutralized before recycling back to the electrolyzer.

Conclusions

Electrolyte composition is known to play an important role in electrochemical processes, and this certainly is the case for the

electroreduction of CO_2 to CO on Ag studied here. We observed that increasing the concentration of the ionic species in the electrolyte (KOH, KCl, and $KHCO_3$) leads to an increase in j_{CO} irrespective of the nature of the anion. j_{CO} values as high as 440 mA cm^{-2} were obtained when using aqueous 3.0 M KOH as the electrolyte. Both R_{ct} and R_{cell} decrease with increasing electrolyte concentration. A decrease in R_{ct} indicates a larger extent of the stabilization of the rate limiting $CO_2^{\bullet-}$ radical. Anions were also found to play a significant role in the process with the onset potential for CO formation shifting in the order $OH^- < HCO_3^- < Cl^-$. The interplay of several factors such as pH, conductivity, and, more importantly, the specific adsorption of certain anions on the electrode surface can be used to explain the various observed phenomena. More rigorous computational efforts or spectro-electrochemical experiments will be needed to further unravel or confirm proposed mechanisms. A deeper understanding of how electrolyte composition affects (and ideally promotes) the electroreduction of CO_2 can guide the design and associated optimum operation conditions of more efficient electro-catalytic systems.

Mixtures of KCl with, respectively, choline Cl, EMIM Cl, or DESs (a 1 : 2 mixture of choline Cl and urea) were also explored because of their potential to enhance CO_2 absorption. Higher j_{CO} values were observed when using these mixtures as the electrolytes compared to when using neat aqueous choline Cl, EMIM Cl, or DESs of equal concentration. These electrolyte mixtures hold promise to be used as a strategy to integrate the processes of CO_2 capture with CO_2 conversion.

Acknowledgements

The authors gratefully acknowledge the financial support from the U.S. Air Force Lab STTR Phase II contract FA8650-14-C-2417 to Dioxide Materials, from the International Institute for Carbon Neutral Energy Research (WPI-I2CNER) sponsored by the Japanese Ministry of Education, Culture, Sports, Science and Technology, and from a 3M graduate fellowship to SV. The authors would also like to thank Dr Huei-Ru ''Molly'' Jhong for stimulating discussions.

Notes and references

1 J. Hansen, P. Kharecha, M. Sato, V. Masson-Delmotte, F. Ackerman, D. J. Beerling, P. J. Hearty, O. Hoegh-Guldberg, S. L. Hsu, C. Parmesan, J. Rockstrom, E. J. Rohling, J. Sachs, P. Smith, K. Steffen, L. Van Susteren, K. von Schuckmann and J. C. Zachos, *PLoS One*, 2013, **8**, e81648.
2 D. R. Feldman, W. D. Collins, P. J. Gero, M. S. Torn, E. J. Mlawer and T. R. Shippert, *Nature*, 2015, **519**, 339–343.
3 S. Pacala and R. Socolow, *Science*, 2004, **305**, 968–972.
4 A. M. Appel, J. E. Bercaw, A. B. Bocarsly, H. Dobbek, D. L. DuBois, M. Dupuis, J. G. Ferry, E. Fujita, R. Hille, P. J. A. Kenis, C. A. Kerfeld, R. H. Morris, C. H. F. Peden, A. R. Portis, S. W. Ragsdale, T. B. Rauchfuss, J. N. H. Reek, L. C. Seefeldt, R. K. Thauer and G. L. Waldrop, *Chem. Rev.*, 2013, **113**, 6621–6658.
5 G. Centi and S. Perathoner, *ChemSusChem*, 2010, **3**, 195–208.
6 H. R. M. Jhong, S. Ma and P. J. A. Kenis, *Curr. Opin. Chem. Eng.*, 2013, **2**, 191–199.
7 D. T. Whipple and P. J. A. Kenis, *J. Phys. Chem. Lett.*, 2010, **1**, 3451–3458.
8 J. A. Herron, J. Kim, A. A. Upadhye, G. W. Huber and C. T. Maravelias, *Energy Environ. Sci.*, 2015, **8**, 126–157.
9 J. L. Qiao, Y. Y. Liu, F. Hong and J. J. Zhang, *Chem. Soc. Rev.*, 2014, **43**, 631–675.
10 Y. Hori, *Modern Aspects of Electrochemistry*, Springer, New York, 2008, pp. 89–189.
11 E. B. Cole, P. S. Lakkaraju, D. M. Rampulla, A. J. Morris, E. Abelev and A. B. Bocarsly, *J. Am. Chem. Soc.*, 2010, **132**, 11539–11551.
12 J. Qu, X. Zhang, Y. Wang and C. Xie, *Electrochim. Acta*, 2005, **50**, 3576–3580.
13 G. Seshadri, C. Lin and A. B. Bocarsly, *J. Electroanal. Chem.*, 1994, **372**, 145–150.
14 D. T. Whipple, E. C. Finke and P. J. A. Kenis, *Electrochem. Solid-State Lett.*, 2010, **13**, B109.
15 S. Zhang, P. Kang and T. J. Meyer, *J. Am. Chem. Soc.*, 2014, **136**, 1734–1737.
16 S. Zhang, P. Kang, S. Ubnoske, M. K. Brennaman, N. Song, R. L. House, J. T. Glass and T. J. Meyer, *J. Am. Chem. Soc.*, 2014, **136**, 7845–7848.
17 Y. Chen and M. W. Kanan, *J. Am. Chem. Soc.*, 2012, **134**, 1986–1989.
18 Y. H. Chen, C. W. Li and M. W. Kanan, *J. Am. Chem. Soc.*, 2012, **134**, 19969–19972.
19 J. L. DiMeglio and J. Rosenthal, *J. Am. Chem. Soc.*, 2013, **135**, 8798–8801.
20 B. Kumar, M. Asadi, D. Pisasale, S. Sinha-Ray, B. A. Rosen, R. Haasch, J. Abiade, A. L. Yarin and A. Salehi-Khojin, *Nat. Commun.*, 2013, **4**, 2819.
21 A. Salehi-Khojin, H. R. M. Jhong, B. A. Rosen, W. Zhu, S. C. Ma, P. J. A. Kenis and R. I. Masel, *J. Phys. Chem. C*, 2013, **117**, 1627–1632.
22 M. Asadi, B. Kumar, A. Behranginia, B. A. Rosen, A. Baskin, N. Repnin, D. Pisasale, P. Phillips, W. Zhu, R. Haasch, R. F. Klie, P. Kral, J. Abiade and A. Salehi-Khojin, *Nat. Commun.*, 2014, **5**, 4470.
23 S. Ma, Y. C. Lan, G. M. J. Perez, S. Moniri and P. J. A. Kenis, *ChemSusChem*, 2014, **7**, 866–874.
24 G. J. Sunley and D. J. Watson, *Catal. Today*, 2000, **58**, 293–307.
25 W. Schneider and W. Diller, *Ullmann's Encyclopedia of Industrial Chemistry*, 2000.
26 I. Ojima, C. Y. Tsai, M. Tzamarioudaki and D. Bonafoux, *Org. React.*, 2000, **56**, 1–354.
27 H. Schulz, *Appl. Catal., A*, 1999, **186**, 3–12.
28 M. E. Dry, *Catal. Today*, 2002, **71**, 227–241.
29 T. Hatsukade, K. P. Kuhl, E. R. Cave, D. N. Abram and T. F. Jaramillo, *Phys. Chem. Chem. Phys.*, 2014, **16**, 13814–13819.
30 K. Chandrasekaran and L. M. Bockris, *Surf. Sci.*, 1987, **185**, 495–514.

31 H. A. Schwarz and R. W. Dodson, *J. Phys. Chem.*, 1989, **93**, 409–414.
32 Y. Hori, H. Wakebe, T. Tsukamoto and O. Koga, *Electrochim. Acta*, 1994, **39**, 1833–1839.
33 C. E. Tornow, M. R. Thorson, S. Ma, A. A. Gewirth and P. J. A. Kenis, *J. Am. Chem. Soc.*, 2012, **134**, 19520–19523.
34 N. Hoshi, M. Kato and Y. Hori, *J. Electroanal. Chem.*, 1997, **440**, 283–286.
35 E. J. Dufek, T. E. Lister and M. E. McIlwain, *J. Appl. Electrochem.*, 2011, **41**, 623–631.
36 E. J. Dufek, T. E. Lister, S. G. Stone and M. E. McIlwain, *J. Electrochem. Soc.*, 2012, **159**, F514–F517.
37 H. R. Jhong, F. R. Brushett and P. J. A. Kenis, *Adv. Energy Mater.*, 2013, **3**, 589–599.
38 B. A. Rosen, A. Salehi-Khojin, M. R. Thorson, W. Zhu, D. T. Whipple, P. J. A. Kenis and R. I. Masel, *Science*, 2011, **334**, 643–644.
39 L. Y. Sun, G. K. Ramesha, P. V. Kamat and J. F. Brennecke, *Langmuir*, 2014, **30**, 6302–6308.
40 W. Zhu, B. A. Rosen, A. Salehi-Khojin and R. I. Masel, *Electrochim. Acta*, 2013, **96**, 18–22.
41 X. P. Zhang, X. C. Zhang, H. F. Dong, Z. J. Zhao, S. J. Zhang and Y. Huang, *Energy Environ. Sci.*, 2012, **5**, 6668–6681.
42 G. Garcia, S. Aparicio, R. Ullah and M. Atilhan, *Energy Fuels*, 2015, **29**, 2616–2644.
43 L. A. Blanchard, D. Hancu, E. J. Beckman and J. F. Brennecke, *Nature*, 1999, **399**, 28–29.
44 M. R. Thorson, K. I. Siil and P. J. A. Kenis, *J. Electrochem. Soc.*, 2013, **160**, F69–F74.
45 Y. Hori, A. Murata and R. Takahashi, *J. Chem. Soc., Faraday Trans. 1*, 1989, **85**, 2309–2326.
46 J. J. Wu, F. G. Risalvato, F. S. Ke, P. J. Pellechia and X. D. Zhou, *J. Electrochem. Soc.*, 2012, **159**, F353–F359.
47 M. S. Naughton, A. A. Moradia and P. J. A. Kenis, *J. Electrochem. Soc.*, 2012, **159**, B761–B769.
48 X. Q. Min and M. W. Kanan, *J. Am. Chem. Soc.*, 2015, **137**, 4701–4708.
49 A. Murata and Y. Hori, *Bull. Chem. Soc. Jpn.*, 1991, **64**, 123–127.
50 R. R. Dogonadz, J. Ulstrup and Y. I. Kharkats, *J. Electroanal. Chem.*, 1972, **39**, 47–61.
51 R. R. Nazmutdinov, D. V. Glukhov, G. A. Tsirlina and O. A. Petrii, *J. Electroanal. Chem.*, 2005, **582**, 118–129.
52 I. Katsounaros and G. Kyriacou, *Electrochim. Acta*, 2007, **52**, 6412–6420.
53 A. J. Bard and L. R. Faulkner, *Electrochemical methods: fundamentals and applications*, Wiley, New York, 2nd edn, 2001.
54 I. S. Kolomnikov and T. V. Lysyak, *Russ. Chem. Rev.*, 1990, **59**, 589–618.
55 J. Paul and F. M. Hoffmann, *Catal. Lett.*, 1988, **1**, 445–455.
56 S. Ma, R. Luo, S. Moniri, Y. C. Lan and P. J. A. Kenis, *J. Electrochem. Soc.*, 2014, **161**, F1124–F1131.
57 E. J. Dufek, T. E. Lister and M. E. McIlwain, *Electrochem. Solid-State Lett.*, 2012, **15**, B48–B50.
58 B. Kim, S. Ma, H. R. M. Jhong and P. J. A. Kenis, *Electrochim. Acta*, 2015, **166**, 271–276.
59 J. S. Spendelow and A. Wieckowski, *Phys. Chem. Chem. Phys.*, 2007, **9**, 2654–2675.
60 O. M. Magnussen, *Chem. Rev.*, 2002, **102**, 679–725.
61 D. D. Bode, *J. Phys. Chem.*, 1972, **76**, 2915–2919.
62 K. L. Hsueh, E. R. Gonzalez and S. Srinivasan, *Electrochim. Acta*, 1983, **28**, 691–697.
63 Y. C. Hsieh, S. D. Senanayake, Y. Zhang, W. Q. Xu and D. E. Polyansky, *ACS Catal.*, 2015, **5**, 5349–5356.
64 S. Lee, D. Kim and J. Lee, *Angew. Chem.*, 2015, **127**, 14914–14918.
65 Y. Hori and S. Suzuki, *J. Electrochem. Soc.*, 1983, **130**, 2387–2390.
66 S. Sowmiah, V. Srinivasadesikan, M. C. Tseng and Y. H. Chu, *Molecules*, 2009, **14**, 3780–3813.

